Low energy (+ and F− ion transmission through condensed layers of water

Mustafa Akbulut, Theodore E. Madey, and Peter Nordlander

Citation: The Journal of Chemical Physics **106**, 2801 (1997); doi: 10.1063/1.473792
View online: http://dx.doi.org/10.1063/1.473792
View Table of Contents: http://scitation.aip.org/content/aip/journal/jcp/106/7?ver=pdfcov
Published by the AIP Publishing

Low energy (<5 eV) F^+ and F^- ion transmission through condensed layers of water

Mustafa Akbulut and Theodore E. Madey[a)]
Department of Physics and Astronomy and Laboratory for Surface Modification, Rutgers, The State University of New Jersey, Piscataway, New Jersey 08855

Peter Nordlander
Department of Physics and Rice Quantum Institute, Rice University, Houston, Texas 77251

(Received 8 August 1996; accepted 12 November 1996)

We report on the transmission of F^+ and F^- ions through ultrathin films of condensed water at 20 K, and compare the experimental results with theoretical calculations. The F^+ and F^- ions are produced by ESD (electron stimulated desorption) of a PF_3 monolayer adsorbed on a Ru(0001) surface (PF_3/Ru(0001) surface). We find two surprising results: (a) the off-normal F^+ signal is attenuated to ~1% by only ~2.5 monolayer (ML) of H_2O, while a much thicker layer, ~10 ML of H_2O, is necessary for equivalent attenuation of the F^- ion emission, and (b) 1 ML of H_2O *increases* the emission of F^- ions and causes a dramatic change in the ion angular distribution. The striking changes in the angular distribution of F^- ions transmitted through condensed H_2O films indicate that elastic scattering is an important process in determining the attenuation of F^- by H_2O. No direct evidence for any kind of ion–molecule chemical reaction or collision induced dissociation reaction has been found. The strong attenuation of F^+ without substantial changes in angular distribution suggests that charge transfer processes are important in limiting the transmission of F^+ ions. Our quantum mechanical calculations indicate that the increase in F^- emission upon adsorption of $\leqslant$1 ML of H_2O is mainly due to a decrease in the neutralization probability of F^- with the substrate, by a dielectric screening mechanism. The calculations also show that the increase in the F^- survival probability saturates after a water bilayer (1 ML H_2O) is formed, which is in excellent agreement with the experiment. Our measurements show no evidence for diffusion of H_2O on the PF_3/Ru(0001) surface between 20 and 60 K; the lack of diffusion, together with exponential attenuation of F^+ and F^- with H_2O thickness, indicates that H_2O vapor condensed on the PF_3/Ru(0001) surface at 20 K grows statistically. © *1997 American Institute of Physics.* [S0021-9606(97)01007-6]

I. INTRODUCTION

Transport of very low energy (<10 eV) ions through water is of importance in many diverse areas such as electrochemistry, radiation chemistry and physics, surface science, and astrophysics.[1–3] In particular, ion transport through liquid water is of fundamental interest in electrochemistry,[1] because water is the most important electrolyte. However, the processes and properties that determine low energy ion transport in H_2O are not yet understood in detail. In order to address fundamental processes (such as energy transfer and charge transfer) that influence ion transport through ultrathin films of atomic and molecular solids, we are systematically studying the transmission of low energy ions through ultrathin films.

We use a new experimental approach to investigate the low energy ion–solid collisions.[4,5] We generate a beam of low energy ions by means of electron stimulated desorption (ESD) from either a compound material such as an oxide or an adsorbed molecular monolayer on a metal surface, which emits ions under electron bombardment. We measure the yield, angular distribution and energy distribution of the ions with a two-dimensional ESDIAD (ESD ion angular distribution) detector at 20 K. We then condense an atomic or a molecular overlayer of known thickness on the surface at 20 K and measure changes in the ESD ion yield, angular distributions and energy distributions as a function of film thickness.

In our first series of experimental studies, we have found that the transmission of low energy positive ions through ultrathin overlayer films depends strongly on the nature of the ion and overlayer materials. ESD- produced $^{16}O^+$ ions (<10 eV) can penetrate Xe and Kr overlayer films several monolayers thick.[4,6,7] In contrast, the $^{16}O^+$ ESD ion emission is suppressed almost completely by ~0.5 ML of condensed water, $H_2\,{}^{18}O$.[5,8] We have attributed the attenuation of $^{16}O^+$ in rare gas films mainly to elastic backscattering; this is supported by a molecular dynamics stimulation by Klein *et al.* which shows that the attenuation in Xe and Kr can be explained by elastic scattering processes.[9] In contrast, the strong attenuation of $^{16}O^+$ in $H_2\,{}^{18}O$ is believed to be due mainly to one-electron charge transfer.

Very recently, we have reported the first study of the transmission of negative ions through ultrathin Xe films.[8,10,11] We have found that one monolayer of Xe increases the emission of F^- ions, whereas additional two monolayers of Xe suppress the F^- signal to 1%. We have suggested that the increase in the F^- signal may be due to a

a)Author to whom correspondence should be addressed; e-mail: madey@physics.rutgers.edu

decrease in the neutralization probability of F^- with the surface.

In this paper, we expand on a preliminary report[12] of the transmission of F^- and F^+ ions through ultrathin condensed H_2O films at 20 K, and compare the experimental findings with the results of quantum mechanical calculations. We generate F^- ions with a peak energy of 1 eV and F^+ ions with a peak energy of 4 eV by means of electron stimulated desorption (ESD) from a chemisorbed PF_3 layer (slightly electron beam damaged) on a Ru(0001) surface, which corresponds to a saturation coverage of PF_3 $\theta_{PF_3} = 0.33$ ML (monolayer). Thus the substrate onto which we dose H_2O is the PF_3/Ru(0001) surface. We have chosen water as an overlayer, since the interaction of H_2O with F^+ and F^- is of fundamental interest in many areas, especially in electrochemistry. We find two very interesting observations: (a) adsorption of $\leqslant 1$ ML of H_2O enhances the F^- ESD ion emission, and (b) thicker films of H_2O attenuate the F^+ signal much more effectively than the F^- signal.[12]

In the next section we describe the experimental procedures and the sample preparation. In Sec. III, we present the experimental results; Sec. III begins with adsorption of water on the PF_3/Ru(0001) and the determination of water coverage, continues with the presentation of the transmission of F^+ and F^- ions through condensed layers of water, and finishes with a study of the diffusion of H_2O on the PF_3/Ru(0001) surface. In Sec. IV, we present a discussion of the experimental results, and present quantum mechanical calculations concerning the enhancement of the F^- emission through water films and compare the results of these calculations with the experiment. Conclusions are given in Sec. V.

II. EXPERIMENTAL PROCEDURES

The experiments are carried out in an ultrahigh vacuum (uhv) chamber (base pressure: $<10^{-8}$ Pa) equipped with instrumentation for surface characterization; details of the apparatus and the methods used have been described previously.[5] The following experiments can be performed in this chamber: (a) thermal desorption spectroscopy (TDS), (b) low energy electron diffraction (LEED), (c) low energy ion scattering (LEIS), (d) Auger electron spectroscopy (AES), and electron stimulated desorption ion angular distribution (ESDIAD) of both positive and negative ions.

The sample, a Ru(0001) crystal, is mounted on a manipulator on which it can be cooled to ~20 K by means of a closed cycle helium refrigerator. The Ru(0001) crystal can be heated in the range 20–1600 K in a controlled way by radiative heating and electron beam heating from a tungsten filament behind the sample. The crystal is cleaned by sputtering using an ~1 keV Ar^+ beam, followed by heating in oxygen to remove the carbon impurities. The oxygen desorbs upon heating the sample to $\geqslant$1600 K. The cleanliness of the sample is checked by AES (Auger electron spectroscopy) and LEED (low energy electron diffraction). The clean Ru(0001) exhibits a (1×1) LEED pattern.

Both F^- and F^+ ions are generated from a slightly electron beam damaged saturation coverage of PF_3 on the Ru(0001) surface, which corresponds to a saturation coverage of PF_3, $\theta_{PF_3} = 0.33$ ML (monolayer). The preparation of the surface is as follows. A saturation coverage of PF_3 is chemisorbed on the clean Ru(0001) surface at ~100 K and then the sample is annealed at 270 K in order to produce an hexagonal array of off-normal ion emission under electron bombardment, for both F^- and F^+ ions. Afterwards the PF_3/Ru(0001) surface is slightly damaged under electron bombardment; ESD of this surface gives rise to a strong F^+ emission normal to the surface, in addition to the hexagonal off-normal beams.[13] The F^- ESDIAD pattern is unchanged by beam damage. The electron-beam damage leads to formation of PF fragments on the surface which are the source of the normal F^+ beam. After these initial surface treatments, the slightly damaged surface remains stable throughout the measurements.

The overlayer gas, H_2O, is purified in several freeze–pump–thaw cycles. H_2O is deposited onto the PF_3/Ru(0001) surface via a leak valve through a directional beam doser aimed at the surface.[5] This procedure permits precise dosing of various coverages of H_2O from fractional monolayer to multilayers.

We use a focused electron beam to initiate ESD processes from a surface area of <1 mm^2 on the PF_3/Ru(0001). During the ESD measurements we use a very low electron fluence ($<2\times10^{13}$ cm^2) in order to minimize electron induced beam damage. By pulsing the electron beam and by gating the high sensitivity digital ESDIAD detector, we can perform time-of-flight (TOF) measurements.[14] This allows us to perform mass, energy, and angle resolved ion detection for both positive and negative ions under appropriate bias and pulse conditions. The TOF capability allows us to separate easily lighter ions (shorter flight times) from heavier ions (longer flight times), and separate negative ions from secondary electrons. For example, using the ESDIAD/TOF detector, we can separate easily H^+, F^+, and CO^+ signals from each other.

We measure the yields and angular distributions of the F^- and F^+ ions from the PF_3/Ru(0001) surface at 20 K with a two-dimensional ESDIAD (ESD ion angular distribution) detector. We then condense an H_2O overlayer of known thickness onto the surface at 20 K and measure changes in the ESD ion yield and angular distributions as a function of film thickness. Our experimental approach is schematically illustrated in Fig. 1.

H_2O is dosed onto the PF_3/Ru(0001) surface at 20 K. As discussed in Sec. III C below, our annealing experiments performed to investigate the growth mode of H_2O on the PF_3/Ru(0001) surface indicate that H_2O adsorbed on the PF_3/Ru(0001) surface at ~20 K grows statistically, and as discussed below, diffuses considerably at temperatures $\geqslant$60 K before desorbing at $T\geqslant$150 K.

The average H_2O thickness is determined using thermal desorption spectroscopy (TDS). Thermal desorption spectra of H_2O from the damaged PF_3/Ru(0001) surface are shown in Fig. 2 and are compared with TDS of H_2O from clean Ru. As seen in Fig. 2, the first H_2O monolayer and subsequent H_2O layers desorb almost at the same temperature, ~160 K,

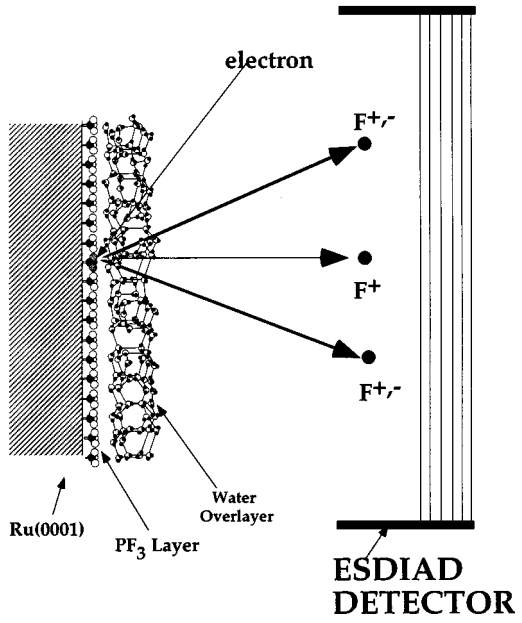

FIG. 1. Schematic of experimental approach.

from the PF_3/Ru(0001) surface; the first layer of H_2O cannot be separated from the subsequent multilayer on the PF_3/Ru(0001) surface. This result indicates that H_2O interacts with PF_3 very weakly.

We identify the coverage corresponding to an H_2O bilayer by TDS of H_2O on clean Ru(0001).[15] Since TDS of H_2O from the Ru(0001) surface is well established, we perform TDS of H_2O from the clean Ru(0001) to determine the coverage of H_2O on the PF_3/Ru(0001). Note that in Fig. 2, the dashed line shows monolayer and multilayer thermal desorption peaks of H_2O from the clean Ru(0001) surface. Assuming that H_2O grows in bilayer form on PF_3/Ru(0001) and defining one monolayer (ML) of H_2O as a complete bilayer, 1 ML corresponds to $\sim 1\times10^{15}$ molecule/cm^2.[15,16] The area integrated H_2O TDS intensity for a monolayer of H_2O on the clean Ru(0001) surface is used to calibrate the coverage of H_2O on the PF_3/Ru(0001) surface.

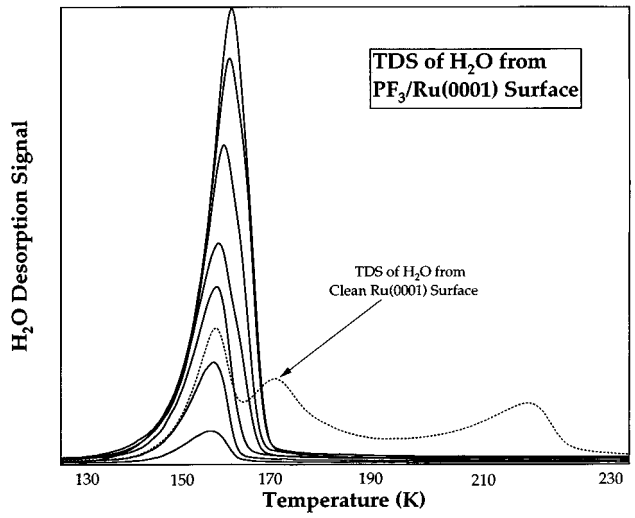

FIG. 2. Thermal desorption spectra (TDS) of H_2O from the PF_3/Ru(0001) surface.

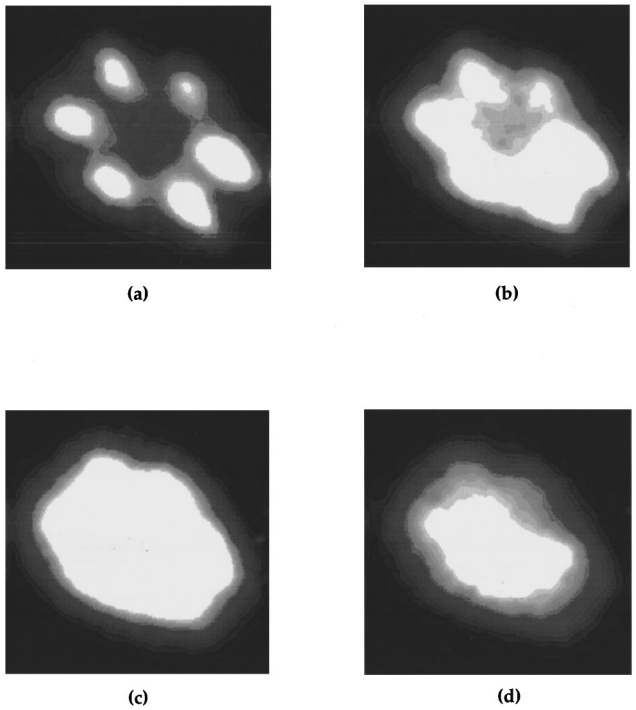

FIG. 3. F^- ESDIAD patterns obtained with a sample bias of -120 V (incident electron energy: 200 eV) from (a) a clean PF_3/Ru(0001) surface at 20 K; (b) $\sim$0.4 ML of H_2O, (c) $\sim$1.0 ML and (d) $\sim$2.0 ML of H_2O adsorbed on PF_3/Ru(0001) surface at 20 K.

III. RESULTS

A. F^- Ion transmission through water layers

Figure 3(a) shows an F^- ESDIAD pattern containing an hexagonal array of off-normal beams from a beam-damaged PF_3/Ru(0001) surface. The hexagonal F^- ESDIAD pattern indicates that PF_3 is azimuthally oriented on the hexagonal Ru substrate. The PF_3 molecules on Ru(0001), which rotate freely about the Ru–P bonds at lower coverages, are constrained azimuthally at saturation coverage in a close-packed $\sqrt{3}\times\sqrt{3}R30°$ array.[10,13,17,18] The hexagonal ESDIAD pattern is believed to be due to equivalent domains of the chemisorbed PF_3 molecules on the hexagonally symmetric Ru surface.

Figures 3(b), 3(c), and 3(d) contain F^- ESDIAD patterns from $\sim$0.4, $\sim$1.0, and 2.0 ML of H_2O adsorbed on the PF_3/Ru(0001) surface, respectively. As seen in Fig. 3(b) and 3(c) adsorption of less than 1 ML of H_2O on the PF_3/Ru(0001) surface increases the F^- ESDIAD intensity. A comparison of Fig. 3(a) with Figs. 3(b) and 3(c) indicates that the increase in F^- emission is accompanied by a dramatic change in the F^- angular distribution: The H_2O overlayer causes the F^- ESDIAD pattern to exhibit a very broad F^- ion angular distribution centered around the surface normal, in addition to the hexagonal beams. As shown in Fig. 3(d), the F^- ESDIAD intensity decreases in the presence of more than 1 ML of H_2O on the PF_3/Ru(0001) surface.

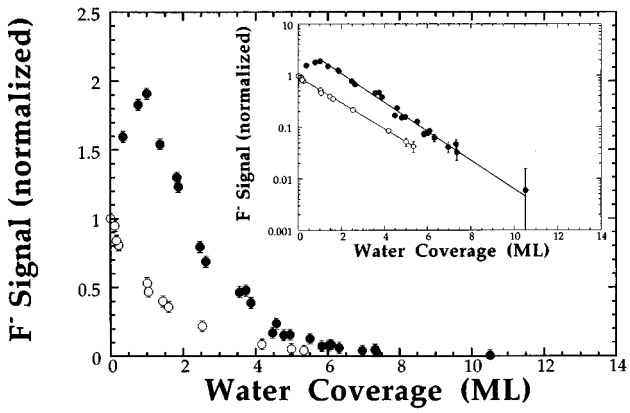

FIG. 4. Total angle-integrated F^- ESD signal from the 1 ML PF_3/Ru(0001) and 10 ML PF_3/Ru(0001) surfaces as a function of H_2O coverage (sample bias: -120 V). The data are normalized to the value of F^- intensity in the absence of H_2O overlayer. In the inset, semilogarithmic plots of the data is shown; line: exponential curve fit. ●: 1 ML PF_3/Ru(0001); ○: 10 ML PF_3/Ru(0001).

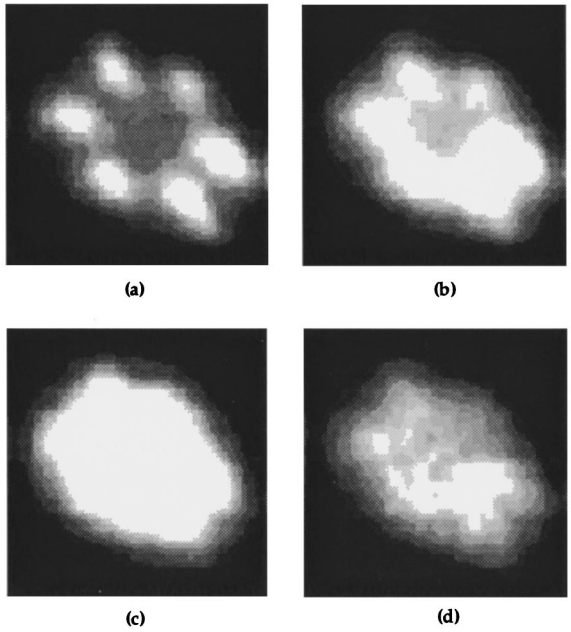

FIG. 5. F^+ ESDIAD pattern obtained with a sample bias of +160 V (incident electron energy: 360 eV) from (a) a clean PF_3/Ru(0001) surface (no H_2O presence); (b) ~0.5 ML of H_2O, (c) ~1.5 ML of H_2O and (d) ~2.8 ML of H_2O adsorbed on PF_3/Ru(0001) surface at 20 K.

The total angle-integrated F^- yield as a function of H_2O film thickness is shown in Fig. 4. It can be seen in Figs. 3 and 4 that in the presence of 1 ML of H_2O the F^- ESDIAD intensity *increases* by a factor of 2. The F^- ESD signal from the PF_3/Ru(0001) surface increases as a function of H_2O coverage up to 1 ML and then decreases for higher H_2O coverages: The F^- signal is attenuated to ~1% by about 10 ML of H_2O.

In order to investigate possible substrate effects on the F^- signal, we have generated a beam of F^- ions from ~10 ML PF_3 adsorbed on the Ru(0001) surface; this PF_3 film is so thick that there is no influence of the Ru substrate on the ion desorption. We condense H_2O films on the 10 ML PF_3/Ru(0001) surface to study the transmission of F^- through water. Figure 4 also shows the total angle-integrated F^- signal generated from a 10 ML thick PF_3 layer as a function of H_2O film thickness. In this case, we find no increase in the F^- emission as a function of H_2O. This observation suggests that the increase in the F^- emission observed in the data of Fig. 4 for 1 ML of PF_3 is related to interactions of F^- with the Ru(0001) surface.

In the inset of Fig. 4, we plot and compare the total angle-integrated F^- signals generated from a 10 ML thick PF_3 layer and from the PF_3/Ru(0001) surface, as a function of H_2O thickness. The attenuation of the F^- signal generated from a 10 ML thick PF_3 layer as a function of H_2O thickness is similar to the attenuation of the F^- signal generated from the PF_3/Ru(0001) surface.

B. F^+ Ion transmission through water layers

Figure 5(a) presents an F^+ ESDIAD pattern from a clean slightly beam damaged PF_3/Ru(0001) surface. The six off-normal F^+ beams originate from the azimuthally oriented PF_3 molecules on the Ru(0001) surface. The sources of the normal F^+ beam in the ESDIAD pattern are the PF fragments formed on the surface by electron-beam damage prior to the ESDIAD measurements.[19]

Figures 5(b)–5(d) show F^+ ESDIAD patterns from the PF_3/Ru(0001) surface covered by ~0.5, ~1.5, and ~2.8 ML of H_2O, respectively. A comparison of Fig. 5(a) with Figs. 5(b)–5(d) indicates that both normal and off-normal F^+ ESDIAD intensities are attenuated, without enhancement, by increasing H_2O coverage. Moreover, inspection of Figs. 5(b)–5(d) indicates that the F^+ ion beam widths do not change significantly after attenuation by the H_2O films. Measurements of the full width at half maximum (FWHM) of the F^+ ion beams as a function of H_2O thickness confirms that the F^+ ion angular widths are not changed significantly in the presence of H_2O overlayer films.

The angle-integrated normal and off-normal F^+ signals as a function of H_2O coverage are shown in Fig. 6 on a linear plot and in the inset of Fig. 6 on a semilogarithmic plot. The attenuation of the off-normal signal is determined by summing the integrated intensity of each of the off-normal beams; the data are normalized to the intensity value at zero H_2O coverage. As seen in Fig. 6, the off-normal beams are attenuated more strongly than the normal beam in passing through the condensed H_2O. As discussed below, this observation can be correlated with the effective attenuation length of the ions in a continuum model.

C. Mobility of water on the PF_3/Ru(0001) surface

To understand better the transmission of ions through condensed H_2O at 20 K, we consider the growth mode of the water films on the PF_3/Ru(0001) surface. The exponential attenuation of both F^+ and F^- yields in H_2O (Figs. 4 and 6) already suggests statistical growth (as a result of limited dif-

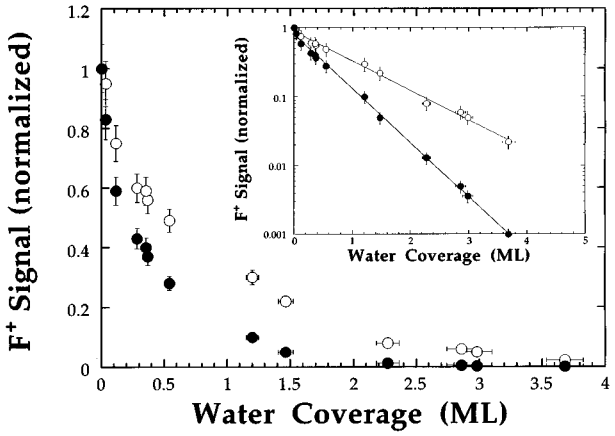

FIG. 6. Normal F^+ and off-normal F^+ ESD signals from the 1 ML PF_3/Ru(0001) surface as a function of H_2O coverage (sample bias: 200 V). In the inset, same data as semilogarithmic plot; line: exponential curve fit. The data are normalized to the value of F^- intensity in the absence of H_2O overlayer. ○: normal F^+ signal; ●: off-normal F^+ signal.

fusion) of H_2O on the PF_3/Ru(0001) at 20 K. In order to verify that diffusion is limited at 20 K, and to determine the onset temperature of diffusion, we have performed a series of annealing experiments. After adsorption of ~1 ML of H_2O on the PF_3/Ru(0001) surface at 20 K, the substrate is successively heated and cooled back down to 20 K, and the F^+ and F^- ESDIAD patterns are measured with the ESDIAD detector.

Figures 7(a) and 7(b) show the F^+ and F^- ESDIAD intensities from ~1-ML H_2O adsorbed PF_3/Ru(0001) surface as a function of annealing temperature, respectively. We find no change in either the F^+ and F^- ESDIAD patterns or their intensities for annealing temperatures between 20 and 60 K. After annealing above 60 K, the F^+ ESDIAD intensity increases, while the F^- ESDIAD intensity decreases. The increase in F^+ signal indicates that there is an increase in the uncovered surface area, which suggests that H_2O vapor condensed on the PF_3/Ru(0001) surface at 20 K does not diffuse, and that adsorbed H_2O molecules diffuse to form 3-dimensional clusters for $T>60$ K. Since the F^- signal increases with H_2O thickness up to 1 ML (see Fig. 3), the decrease in the F^- intensity during annealing to $T>60$ K also indicates an increase in the uncovered surface area.

D. Work function measurements

In order to investigate the effects of work function on the F^- signal in the presence of a water overlayer, we measure the work function of the PF_3/Ru(0001) surface as a function of H_2O thickness.

We generate a secondary electron yield by bombarding the substrate with a focused 3 keV electron beam. Typical electron fluences are of the order of 5×10^{14} cm^{-2}; no evidence for beam damage is observed. By measuring the low energy cutoff of the secondary electron yield as a function of water thickness using a concentric hemispherical analyzer (CHA), we determine the change in the work function as a function of water thickness. We assume that the work function of clean Ru(0001) is about 5.52 eV.[20] Chemisorption of ~1 ML PF_3 increases the work function about 0.5 eV. Adsorption of H_2O on the PF_3/Ru(0001) surface leads to a decrease in the work function. As seen in Fig. 8, upon ad-

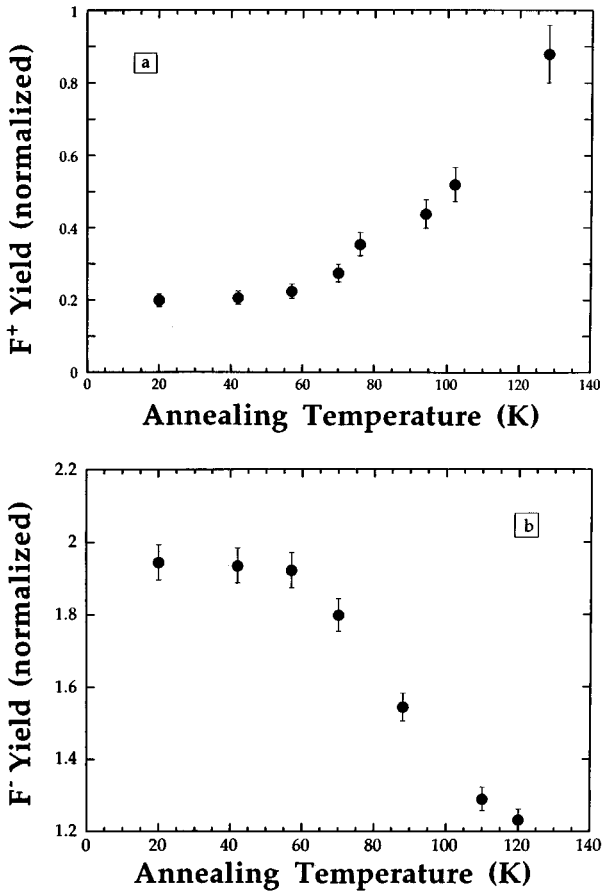

FIG. 7. (a) Total angle-integrated F^+ ESDIAD intensity in the 20–130 K annealing temperature range for ~1 ML of H_2O on the PF_3/Ru(0001) surface. (b) Total angle-integrated F^- ESDIAD intensity in the 20–130 K annealing temperature range for ~1 ML of H_2O on the PF_3/Ru(0001) surface.

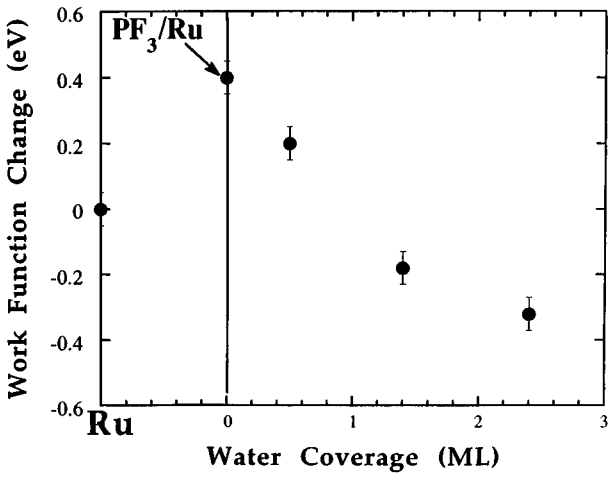

FIG. 8. Changes in the work function as a function of H_2O overlayer thickness, as derived from the onset energy of the secondary electron emission.

sorption of 1 ML of H_2O on the PF_3/Ru(0001) surface, the work function decreases about 0.5 eV with respect to the work function of the PF_3/Ru(0001) substrate.

IV. DISCUSSION

A. Growth mode and mobility of water on the PF_3/Ru(0001) surface

Before discussing the transmission of F^+ and F^- through condensed water at 20 K, we first consider the growth mode of the water films on the PF_3/Ru(0001) surface at 20 K. The important question is whether water vapor condensed on the PF_3/Ru(0001) surface at 20 K diffuses to form 3-dimensional clusters. Our annealing experiments to investigate mobility of H_2O on the PF_3/Ru(0001) surface show that both F^+ and F^- ESDIAD intensities from the 1 ML H_2O adsorbed PF_3/Ru(0001) surface remain unchanged upon annealing between 20 and 60 K; above 60 K, the F^+ ESDIAD intensity increases while the F^- intensity decreases. The increase in F^+ signal and the decrease in the F^- signal above 60 K indicate that there is an increase in the uncovered surface area, which show evidence for surface diffusion of H_2O for $T>60$ K. Based on these data, we suggest that H_2O vapor condensed on the PF_3/Ru(0001) surface at 20 K grows so as to hinder the formation of 3-dimensional water clusters by diffusion[21] (although we cannot rule out the possibility of short range transient diffusion during adsorption). This observation, coupled with the exponential attenuation of both positive and negative F ions in H_2O as a function of thickness, supports the interpretation that H_2O films grow statistically upon adsorption at 20 K, and that diffusion to form clusters occurs for $T>60$ K.

We can estimate roughly the diffusion energy of H_2O monomers on the PF_3/Ru(0001) surface by using a single atom diffusion model[22]

$$D=\frac{1}{2}\nu a^2 \exp\left(-\frac{E_{\mathrm{diff}}}{RT}\right) \tag{1}$$

with

$$[\langle x^2\rangle]^{1/2}=(2D\Delta t)^{1/2}. \tag{2}$$

Here, ν is the jump attempt frequency of a monomer, a is the jump length, E_{diff} the diffusion (activation) energy, $[\langle x^2\rangle]^{1/2}$ is the root-mean-square average jump distance, and Δt is the average jump time. Assuming that $\Delta t\approx 10$ s, $a\approx 3$ Å, $x\approx 10$ Å, $\nu\approx 10^{12}$ s^{-1}, we can estimate E_{diff} to be ~0.16 eV (~15 kJ/mol) for 70 K. This value, which is relatively insensitive to the choice of parameters, corresponds to ~30% of the desorption energy of H_2O [~0.5 eV (~50 kJ/mol) for desorption at ~150 K]. It is generally expected that diffusion energies for adsorbates are approximately 10% to 40% of the desorption energy,[22,23] so that our estimated diffusion energy for H_2O on the PF_3/Ru(0001) surface is physically reasonable.

Water vapor condensed on the PF_3/Ru(0001) surface at 20 K is expected to form amorphous solid water (ice). It has been reported that the structure of the amorphous ice has oxygen–oxygen nearest-neighbor tetrahedral symmetry, on average.[24] We expect that the amorphous ice overlayer has a very open structure with disordered hexagonal H-bonded rings. Since the range of the interaction potential for the F^-–H_2O interaction is very short[25] [for ~3 eV F^-, R(O–F) ≈1.7 Å] compared with the lengths of the space lattice of ice (>4.4 Å)[26] the ions may easily penetrate several layers of H_2O. Therefore, we believe that the structure of the ice films plays a very important role in the ion transmission.

In the following, we first discuss the possible mechanisms for the enhancement of the F^- signal and then discuss the attenuation of the F^- and F^+ signals in the condensed water films in terms of elastic and inelastic scattering, and charge transfer processes.

B. Enhancement of the F^- signal

Several different mechanisms by which the F^- signal could be enhanced due to adsorption of ⩽1 ML of H_2O are (a) increase in the initial excitation probability upon adsorption of H_2O, (b) charge transfer from H_2O to the desorbing F^+ ion and neutral F to form F^- ions, and (c) decrease in the neutralization probability of the desorbing F^- ions with the Ru substrate. An important question related to these processes is whether or not the Ru substrate plays an important role in the enhancement of the F^- signal.

Based on the observations in Sec. III A, we can eliminate charge transfer from H_2O to the desorbing species as potential cause of the F^- emission enhancement. The absence of an increase in the F^- emission from the thick PF_3 film through H_2O indicates that charge transfer from H_2O to the desorbing species to form F^- ions is not a dominant process.

Now let us consider how the substrate could influence the negative ion desorption. It is well known that the neutralization probability of desorbing negative ions is very high in the vicinity of a surface.[27–30] The increase in F^- signal could be due to a decrease in the resonant tunneling rate of an electron from an F^- ion to the Ru(0001) surface caused by adsorption of H_2O. A change in the work function[31] and dielectric screening upon adsorption of H_2O as well as the polarization force induced in the water overlayer could affect the resonant tunneling probability.

Our measurements (Sec. III D and Fig. 8) show that adsorption of H_2O on the PF_3/Ru(0001) surface reduces the work function. However, the work function decreases only ~0.5 eV relative to the work function of PF_3/Ru(0001) for 1 ML of H_2O. Since the work function of PF_3/Ru(0001) is ~5.8 eV and the electron affinity of fluorine is ~3.4 eV, the decrease in the work function upon adsorption of 1 ML of H_2O is not expected to change the resonance tunneling rate significantly.[31] Recently, we have found that the F^- signal from the PF_3/Ru(0001) surface increases by a factor of 4 in the presence of 1 ML of Xe.[8] For the 1 ML Xe covered PF_3/Ru(0001) surface, the work function decreases only about 0.07 eV relative to the work function of PF_3/Ru(0001) system. This very small decrease cannot explain the fourfold increase in the F^- yield upon adsorption of 1 ML of Xe. Therefore, we do not believe that the decrease in the work

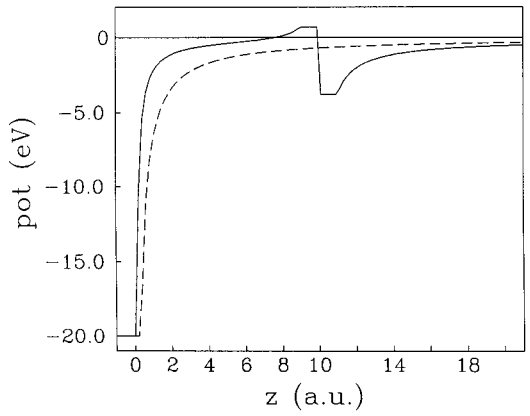

FIG. 9. The solid line shows the potential energy of an electron as a function of distance z from a metallic surface covered by a dielectric layer of thickness $d=10$ a.u. and dielectric constant of $\mathscr{E}=3$. The dashed line shows the potential energy for an electron outside a bare metal surface. The distance z is in a.u. and measured from the metal surface.

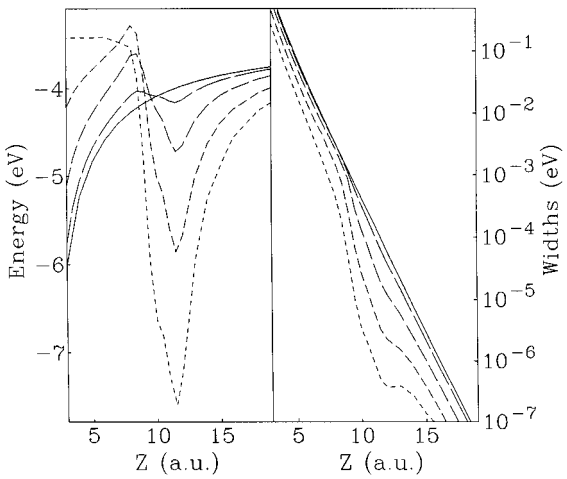

FIG. 10. Energy shift and broadening of the F^- ($m=0$) level as a function of atom–metal surface separation Z outside a metallic surface covered by a dielectric film of thickness $d=10$ a.u. The solid line is for $\mathscr{E}=1$ (vacuum), the long-dashed line for $\mathscr{E}=1.1$, the dashed line is for $\mathscr{E}=1.5$, the short-dashed line is for $\mathscr{E}=3$ and the dotted line is for $\mathscr{E}=40$. The distance Z is in a.u. and is measured from the metal surface.

function is the main reason for the enhancement of the F^- signal.

Another possibility is that the F^- signal enhancement is due to dielectric screening caused by the H_2O film. In order to estimate the effects of the dielectric overlayer on the electron tunneling rates between an ion and the metal, we have calculated the energy shift and broadening of a negative F ion outside a metal surface covered by a thin dielectric film using the complex scaling method.[32,33] The water overlayer has been modeled as a uniform dielectric film with dielectric constant $\mathscr{E}$ and thickness d. Within such a model, the initial adsorption of water on Ru(0001) leading to the first monolayer is described assuming a constant film thickness but with a gradual increase of the dielectric constant from that of water vapor $\mathscr{E}=1.01$ to something of the same order as or less than the dielectric constant of ice, $\mathscr{E}=80$. Since the dielectric constant of a thin water film adsorbed on a metal surface is unknown, the results of the investigation are at a qualitative level.

The electrostatic potential in the system was calculated by matching the solutions to Poisson's equation in the metal (which for simplicity is treated as a perfect conductor), the dielectric film, and the vacuum region to each other using the proper boundary conditions.[34] The image potential of the metal has been truncated at a distance corresponding to an image attraction of -20 V, which is equal to the bulk potential of a typical free electron metal. (Note that the truncation does not affect the calculated parameters.) Since the dielectric screening in the water film is mediated by the alignment of individual water molecules, the electrostatic potential in the dielectric film was truncated and assumed constant within a distance $Z_{\mathrm{mol}}\approx 1$ a.u. from the dielectric interfaces. The calculated tunneling rates are not sensitive to variations of the truncation distance in the interval $0<Z_{\mathrm{mol}}<2$ a.u.

In Fig. 9, we show the electrostatic potential energy for an electron outside the metal covered by a dielectric film of thickness 10 a.u. For comparison, we also show the potential outside the bare metal. It can be seen that weak imagelike potentials are induced near the interfaces of the dielectric film. Close to the interfaces, these potentials are similar to what would be expected near the interface of two semi-infinite dielectric slabs. From the figure it is clear that the presence of the dielectric film introduces a potential barrier between an atom and the metal surface. This potential barrier will decrease electron tunneling rates near the surface.

The shift and broadening of the F^- level can be calculated using the complex scaling method by solving the Schroedinger equation in the calculated electrostatic potential. In Fig. 10, the shifts and widths of an F^- level as a function of atom–metal separation Z is shown for dielectric films of different constants. The figure shows large shifts of the negative ion level near the vacuum-film interface. These shifts follow the local variation of the electrostatic potential shown in Fig. 9. It can be seen that for all atom–surface separations, the widths decrease with increasing dielectric constant. The decrease of the widths is largest when the atom is just outside the dielectric film. This is caused by the relatively large down shift of the negative ion state near the vacuum-film interface, which results in an enhanced potential barrier between the atom and the metal surface. As the dielectric constant increases, the electrostatic potential in the dielectric film approaches a simple rectangular barrier and the width eventually saturates. For dielectric constants larger than 10, the calculated widths as functions of atom–surface separation are essentially independent of $\mathscr{E}$.

In order to model the charge transfer dynamics, we have calculated the population of the F^- during desorption through the thin film using a simple Anderson model ($U=0$).[35] The fluorine is assumed to start as a negative ion at an atom–surface separation $Z=4.5$ a.u. and move in the vacuum direction with a kinetic energy 1 eV. In Fig. 11, we plot the instantaneous negative ion population of F^- during desorption through films of different dielectric constants.

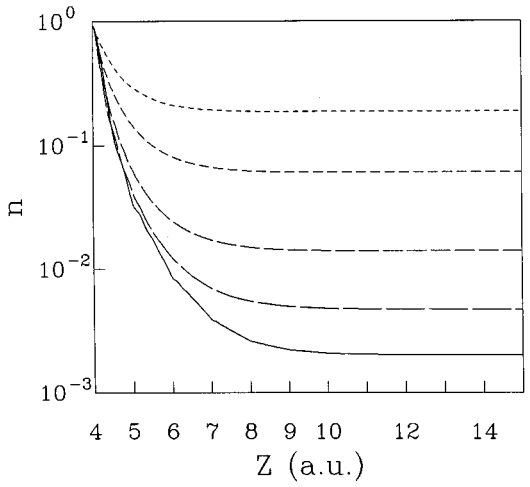

FIG. 11. Instantaneous negative ion population as a function of atom-metal surface separation Z during desorption of F^- through a dielectric thin film. The solid line is for $\mathscr{E}=1$ (vacuum), the long-dashed line for $\mathscr{E}=1.1$, the dashed line is for $\mathscr{E}=1.5$, the short-dashed line is for $\mathscr{E}=3$ and the dotted line is for $\mathscr{E}=40$. The distance Z is in a.u. and measured from the metal surface.

The figure shows that the presence of the film increases the survival probability of F^- significantly. This conclusion does not depend on the assumptions regarding to the atomic trajectory and kinetic energy. The figure also shows that no neutralization of F^- occurs for larger atom–metal separations Z than 8 a.u. The increase in the survival probability of the F^- therefore saturates after a monolayer is formed, which is in excellent agreement with the experiment.

These calculations, although of qualitative nature, clearly demonstrate the importance of dielectric screening in reducing the neutralization probability of an F^- desorbing through a thin dielectric film. A detailed quantitative analysis of the experiment would require going beyond the jellium description of the condensed overlayer and taking into account both the electronic and ionic screening. At present, this represents an impossible task.

C. Attenuation of F^- and F^+ in water

A comparison of the F^+ signal with the F^- signal as a function of H_2O thickness indicates that the F^+ signal is attenuated much more effectively by H_2O than the F^- signal and that the F^- ions can penetrate H_2O overlayers several monolayers thick. As seen in Figs. 4 and 6, the attenuations of the F^- and F^+ are exponential, and we can derive average attenuation thicknesses (lengths) λ of the ions. We define λ as the average overlayer thickness that attenuates the ion signal to e^{-1} (0.368) of the initial value. From Figs. 4 and 6, we find the average attenuation length, λ, for F^+ and F^- in H_2O to be

$$\lambda \approx 0.42 \text{ ML} \cong 1.56 \text{ Å} \quad \text{for off-normal } F^+,$$
$$\lambda \approx 0.85 \text{ ML} \cong 3.16 \text{ Å} \quad \text{for normal } F^+,$$
$$\lambda \approx 1.63 \text{ ML} \cong 5.22 \text{ Å} \quad \text{for total } F^-.$$

Assuming a continuum model, the relative attenuation of the off-normal and normal F^+ signals can be correlated with the effective escape depth of the ions, λ, in the condensed water. This is defined as $\lambda=\lambda_0 \cos\varphi$, where φ is the angle that a desorbing ion makes from the surface normal, and λ_0 is 3.16 Å for F^+. Since the off-normal ions desorb with angles $\varphi \sim 60°$ with respect to surface normal, the off-normal F^+ signal should be attenuated ~ 2 times stronger than the normal F^+ signal which is in very good agreement with our experimental results.

Defining the collision cross section as $\sigma=1/N\lambda_0$ ($N=3.2\times10^{22}$ molecule/cm^3),[26] we can calculate the collision cross sections, σ, for F^+ and F^- in H_2O to be

$$\sigma=(1.0\pm0.2)\times10^{-15} \text{ cm}^2 \quad \text{for } F^+,$$
$$\sigma=(6.0\pm0.8)\times10^{-16} \text{ cm}^2 \quad \text{for } F^-.$$

We now discuss the relative attenuation of F^- and F^+ ions in the H_2O films. We address first the evidence for elastic scattering and then address charge transfer.

1. Attenuation of F^- in water

Collisions of negative ions with neutral molecules on or near a surface can lead to detachment of the loosely bound electron in several distinct ways. The image potential shifts the electron affinities of fluorine and H_2O down in energy (i.e., larger value of affinities); we expect that the relative difference is very small. A negative H_2O ion may be formed near a surface (the electron affinity of a free H_2O molecule is ~ 0.0001 eV[36]); however, the charge exchange reaction

$$F^- + H_2O \rightarrow F + H_2O^- \quad (\Delta E = +3.40 \text{ eV}) \tag{1}$$

is endothermic and is not likely to occur in low energy (~ 1 eV) collisions near the surface. Moreover, in amorphous ice the bottom of the conduction band lies ~ 0.8–1.0 eV below the vacuum level:[37] The charge transfer reaction between F^- and the ice film is expected to be endothermic by ~ 2.4 eV. For the $F^- + H_2O$ system, the following electron detachment and dissociative attachment reactions could be also possible:

$$F^- + H_2O \rightarrow F + H + OH^- \quad (\Delta E = +6.77 \text{ eV}), \tag{2}$$

$$F^- + H_2O \rightarrow HF + OH + e^- \quad (\Delta E = +2.80 \text{ eV}), \tag{3}$$

and

$$F^- + H_2O \rightarrow HF + OH^- \quad (\Delta E = +0.95 \text{ eV}). \tag{4}$$

All these reactions are endothermic (the gas phase endothermicities for ground-state reactants and products are listed along with each reaction channel). Although reaction (4) seems to be possible, we expect a relatively small cross section ($<10^{-16}$ cm^2) for the interaction of a low energy F^- ion with an H_2O molecule via reaction (4),[38] because the most probable kinetic energy of the F^- ion (~ 1 eV) is very close to the threshold energy of the reaction ($+0.95$ eV). Therefore, we do not consider that any of these reactions is an important collision channel in our experiment.

We suggest that the cross section for interaction of ~ 1 eV F^- with H_2O is low because the electron detachment processes have low probability, and because of the open structure of the ice films. Due to the hydrogen bonded network structure, the ice films are expected to contain intersti-

tial regions ($\sim$24 Å^2 in area)[1,26,39] which are larger than the dimensions of an F^- ion ($\sim$6 Å^2 in area; the radius of F^- is 1.36 Å). This appears to be the main reason why some F^- ions penetrate ice films 10 ML thick.

We suggest that the attenuation of F^- is mainly due to multiple elastic and inelastic (such as ion–phonon and dielectric relaxation) scattering that eventually stops the ions penetrating through the water films. In the condensed molecular media, a moving F^- ion can interact with the lattice vibration (phonon) modes and can lose a small fraction of its energy to the elastic continuum. Since water is a dipolar substance, it is also possible that the F^- ions can lose energy to dipolar relaxation.[40]

The elastic scattering process can be a single binary collision or a series of binary collisions between a desorbing ion and lattice H_2O molecules. If the F^- ion is scattered in the forward direction it may ''channel'' through the interstitial regions of the ice film and escape from the condensed H_2O overlayer. However, in the case of scattering by an angle of 90° or more with respect to the surface normal as a result of a series of binary collisions, we do not expect that the ion can escape from the overlayer films after losing sufficient energy; it may become trapped in the ice films as a result of ion–solvent (water) interactions, or become neutralized by charge transfer at the film–solid interface. Since amorphous solid ice can serve as a useful model of liquid water,[1,24] the transport of low energy F^- ions through amorphous ice films has very important implication in electrochemistry.

If the kinetic energy of an F^- ion is close to zero, the time an F^- spends near a water molecule is long compared with the average time a water molecule takes to orient into association with an ion. In this case, the ion–dipole forces may cause some of the water molecules to break away from the ice network and attach themselves to the ions to trap it. This requires a large reorientation in the ice films (the heat of solvation for F^- in liquid H_2O is $\sim$4.3 eV).[1]

2. Attenuation of F^+ in water

As seen in Figs. 5 and 6, the F^+ signal from the PF_3/Ru(0001) decreases as a function of H_2O thickness. This indicates that dielectric screening does not affect neutralization of a positive ion significantly. We can explain this result considering the energy levels of an F^+ ion. The unoccupied state (ionization level: $\sim$17.4 eV) of F^+ is located well below the PF_3/Ru valence band ($E_f \approx 5.9$ eV and conduction band width is $\sim$5 eV). Therefore, the neutralization of positive fluorine ions by the surface is mainly due to Auger neutralization processes. Since F^+ ions do not undergo charge transfer by resonance electron tunneling, we expect that dielectric screening does not have a strong influence on the F^+ desorption probability from the surface.

It may appear surprising that H_2O attenuates the F^+ signal much more effectively than the F^- signal. Considering only a simple hard-sphere elastic scattering model, one expects that the F^- signal would be attenuated more strongly than the F^+ signal in H_2O, because the ionic radius of F^- ($\sim$1.36 Å) is larger than that of F^+ ($\sim$0.8 Å). Based on this simple model, we suggest that elastic scattering processes should *not* be the dominant processes determining the attenuation of F^+ ions by H_2O. In fact, the experimentally observed attenuation of F^+ without substantial changes in angular distributions (Figs. 5 and 6) also supports the interpretation that elastic scattering processes are not dominant in the attenuation of F^+ in H_2O films.

If elastic scattering processes are not the main reasons for the attenuation of the F^+ signal, we consider other possibilities, i.e., ion–molecule reactions and charge transfer processes to explain the strong attenuation of the F^+ signal compared to the F^- signal in H_2O.

The ion–molecule reactions

$$F^+ + H_2O \rightarrow (HF)^+ + OH, \tag{5}$$

$$F^+ + H_2O \rightarrow HF + (OH)^+ \tag{6}$$

are possible in our experiments, because reaction (5) and reaction (6) are expected to be exoergic by $\sim$2.2 and $\sim$4.8 eV, respectively. Although these processes are energetically possible and may actually occur in the film, our measurements show no direct evidence for these ion–molecule reactions; i.e., we do not detect any ionic reaction products among the desorbing ions.

Let us now consider charge transfer processes. In a one-electron charge transfer reaction an ion captures an electron from a target molecule and becomes a neutral.[5,41] In a charge transfer reaction, the energy defect, ΔE, (the total internal energy change) is an important parameter governing the charge transfer at low energy ($<$10 eV), and provides intuitive knowledge about the reactions. At low relative kinetic energy ($<$10 eV), the charge transfer cross section depends strongly on whether a reaction is exothermic or endothermic. For exothermic reactions, the ion-molecule charge transfer cross sections are generally very large (10^{-14}–10^{-15} cm^2) at low energies ($<$10 eV).[42] In the gas phase, the charge transfer reaction

$$F^+ + H_2O \rightarrow F + (H_2O)^+ \tag{7}$$

is exoergic by $\sim$4.8 eV. We expect that in the vicinity of the surface the ionization energies of fluorine and water shift up in energy due to image potential effects; the relative ionization energies are not expected to change significantly. Hence, charge transfer is an energetically possible reaction channel during F^+ ion transmission through the H_2O films.

Experimental and theoretical studies of gas-phase charge transfer collisions indicates that the smaller the energy defect, the larger the charge transfer probability.[42,43] Based on our earlier work[5,11] and the present study, we find a similar correlation between the energy defects and the measured attenuation cross sections. Adsorption of only 0.5 ML of $H_2\,{}^{18}O$ onto an ^{16}O-oxidized W substrate is enough to suppress the $^{16}O^+$ ion emission by a factor of 100, while three monolayers of NH_3 are necessary for equivalent suppression of the $^{16}O^+$ ion emission. As discussed in detail in Ref. 5, the attenuation of $^{16}O^+$ by $H_2\,{}^{18}O$ and NH_3 is attributed mainly to one-electron charge transfer neutralization. The measured $^{16}O^+$ attenuation cross sections are $\sim 9\times10^{-15}$ cm^2 for

$H_2\,{}^{18}O$ and $\sim 3\times 10^{-15}$ cm^2 and NH_3. In the gas phase, for one-electron charge transfer reactions between O^+ and H_2O, and between O^+ and NH_3, the energy defects are 1 and 2.2 eV, respectively; both reactions are exothermic. As discussed above, the cross section for attenuation of F^+ by H_2O is $\sim 1.0\times 10^{-15}$ cm^2, and the gas phase energy defect is $\sim$4.8 eV exoergic. A comparison of our measured attenuation cross sections with the energy defects for the charge transfer reactions reveals that the smaller the energy defect, the larger the attenuation cross section.

V. CONCLUSIONS

We have found that charge transfer and elastic scattering processes determine the transmission of ESD-produced low energy ions ($\sim$4 eV F^+ and $\sim$1 eV F^-) through ultrathin films of condensed water. Surprisingly, low energy ($\sim$1 eV) F^- ions undergo a striking change in desorption angular distributions and can penetrate many layers of a condensed water films; this observation is attributed mainly to elastic and inelastic scattering. Since the electron detachment and dissociative attachment processes are highly endothermic for the F^-–H_2O system, we believe that even at thermal energies the dominant interaction between an F^- ion and a H_2O layer is scattering without charge transfer. In contrast, the strong attenuation of F^+ without substantial changes in angular distribution suggests that charge transfer processes are important in this case. Since amorphous solid ice can serve as a useful model of liquid water, the transport of low energy negative and positive ions through amorphous ice films has very important implication in electrochemistry. Our finding can provide insights into the ion–solvent interactions in electrochemistry. Based on a calculation using the complex scaling method, we attribute the enhancement of the F^- upon adsorption of a monolayer of water mainly to a dielectric screening mechanism, which decreases the neutralization probability of the desorbing F^- with the substrate.

ACKNOWLEDGMENTS

This work is supported in part by the National Science Foundation, Grants Nos. CHE-9408367 and DMR 95-21444.

[1] J. O. Bockris and A. K. N. Reddy, *Modern Electrochemistry 1 & 2* (Plenum, New York, 1970).
[2] L. Sanche, in *Linking the Gaseous and Condensed Phases of Matter*, edited by L. G. Christophorou, E. Illenberger, and W. F. Schmidt. (Plenum, New York, 1994), p. 31.
[3] P. Sigmund, M. T. Robinson, and M. S. Baskes, Nucl. Instrum. Methods Phys. Res. B **36**, 110 (1989).
[4] N. J. Sack, M. Akbulut, and T. E. Madey, Phys. Rev. Lett. **73**, 794 (1994).
[5] M. Akbulut, N. J. Sack, and T. E. Madey, J. Chem. Phys. **103**, 2202 (1995).
[6] N. J. Sack, M. Akbulut, and T. E. Madey, Phys. Rev. B **51**, 4585 (1995).
[7] N. J. Sack, M. Akbulut, and T. E. Madey, Nucl. Instrum. Methods Phys. Res. B **90**, (1994).
[8] N. J. Sack, M. Akbulut, and T. E. Madey, Surf. Sci. Lett. **334**, L695 (1995).
[9] P. Klein, M. Vicanek, and H. Urbassek, Phys. Rev. B **51**, 4597 (1995).
[10] N. J. Sack, M. Akbulut, T. E. Madey, P. Klein, H. M. Urbassek, and M. Vicanek, Phys. Rev. B **54**, 5130 (1996).
[11] T. E. Madey, N. J. Sack, and M. Akbulut, Nucl. Instrum. Methods Phys. Res. B **100**, 309 (1995).
[12] M. Akbulut, N. J. Sack, and T. E. Madey, Phys. Rev. Lett. **75**, 3414 (1995).
[13] A. L. Johnson, S. A. Joyce, and T. E. Madey, Phys. Rev. Lett. **61**, 2578 (1988).
[14] T. E. Madey, S.E. Joyce, and C. Benndorf, in *Physics and Chemistry of Alkali Metal Adsorption*, edited by H. P. Bonzel, A. M. Bradshaw, and G. Ertl. (Elsevier Science, New York, 1989), p. 185.
[15] D. L. Doering and T. E. Madey, Surf. Sci. **123**, 305 (1982).
[16] G. Pirug, C. Ritke, and H. P. Bonzel, Surf. Sci. **241**, 289 (1991).
[17] T. E. Madey, H.-S. Tao, L. Nair, U. Diebold, S. M. Shivaprasad, A. L. Johnson, A. Poradzisz, N. D. Shinn, J. A. Yarmoff, and V. Chakarian, in *Desorption Induced by Electron Transitions DIET V*, edited by A. R. Burns, E. B. Stechel, and D. R. Jennison. (Springer, Berlin, 1993) p. 182.
[18] N. J. Sack and T. E. Madey, Surf. Sci. **347**, 367 (1996).
[19] L. Nair, Ph.D. thesis, Rutgers University, 1994.
[20] V. Chakarian, D. K. Shuh, J. A. Yarmoff, H.-S. Tao, U. Diebold, B. L. Maschhoff, and T. E. Madey, J. Chem. Phys. **100**, 5301 (1994).
[21] M. Akbulut, N. J. Sack, and T. E. Madey, Surf. Sci. **351**, 209 (1996).
[22] R. Gomer, Rep. Prog. Phys. **53**, 917 (1990).
[23] P. A. Thiel and T. E. Madey, Surf. Sci. Rpt. **7**, 211 (1987).
[24] A. H. Narten, C. G. Venkatesh, and S. A. Rice, J. Chem. Phys. **64**, 1106 (1976).
[25] H. Kistenmacher, H. Popkie, and E. Clementi, J. Chem. Phys. **58**, 5627 (1973).
[26] P. V. Hobbs, *Ice Physics* (Clarendon, Oxford, 1974).
[27] P. Nordlander and J. C. Tully, Phy. Rev. Lett. **61**, 990 (1988).
[28] P. Nordlander, Scanning Microscopy Suppl. 3, 353 (1990).
[29] J. C. Tully, Phys. Rev. B **16**, 4324 (1977).
[30] M. L. Yu and N. D. Lang, Nucl. Instrum. Methods Phys. Res. B **14**, 403 (1986).
[31] S. A. Joyce, C. Clark, V. Chakarian, D. K. Shuh, J. A. Yarmoff, T. E. Madey, P. Nordlander, B. L. Maschhoff, and H. S. Tao, Phys. Rev. B **45**, 14264 (1992).
[32] P. Nordlander and J. C. Tully, Phys. Rev. B **42**, 5564 (1990).
[33] P. Nordlander, Phys. Rev. B **46**, 2584 (1992).
[34] P. Nordlander and J. Modisette (unpublished).
[35] H. Shao, D. C. Langreth, and P. Nordlander, in *Low Energy Ion–Surface Interactions*, edited by J. W. Rabalais. (Wiley, New York, 1994), p. 118.
[36] L. G. Christophorou, D. L. McCorkle, and A. A. Christodoulides, in *Electron–Molecule Interactions and Their Applications*, edited by L. G. Christophorou (Academic, Orlando, 1984), p. 424.
[37] M. Michaud, P. Cloutier, and L. Sanche, Phys. Rev. A **44**, 5624 (1991).
[38] R. D. Levine and R. B. Bernstein, *Molecular Reaction Dynamics and Chemical Reactivity* (Oxford University Press, New York, 1987).
[39] N. H. Fletcher, *The Chemical Physics of Ice* (Cambridge University Press, Cambridge, 1970).
[40] H. Frohlich, Phys. Rev. **92**, 1152 (1953).
[41] E. W. McDaniel, J. B. A. Mitchell, and M. E. Rudd, *Atomic Collisions: Heavy Particle Projectiles* (Wiley-Interscience, New York, 1993).
[42] F. Linder, in *Electronic and Atomic Collisions*, edited by H. B. Gilbody, W. R. Newell, F. H. Read, and A. C. H. Smith (Elsevier Science, New York, 1988), p. 287.
[43] D. Rapp and W. E. Francis, J. Chem. Phys. **37**, 2631 (1962).